2014

Behavior of I-Section GFRP Beam Including Retrofitting for Damage Effects

Mamadou Konate
Old Dominion University

Zia Razzaq
Old Dominion University, zrazzaq@odu.edu

Original Publication Citation
Mamadou, K., Mamadou, K., & Zia, R. (2014). Behavior of I-section GFRP beam including retrofitting for damage effects. *Global Journals of Research in Engineering*, *14*(E6), 1-5. https://engineeringresearch.org/index.php/GJRE/article/view/1208

Global Journal of Researches in Engineering: E
Civil And Structural Engineering
Volume 14 Issue 6 Version 1.0 Year 2014
Type: Double Blind Peer Reviewed International Research Journal
Publisher: Global Journals Inc. (USA)
Online ISSN: 2249-4596 & Print ISSN: 0975-5861

Behavior of I-Section GFRP Beam Including Retrofitting for Damage Effects

By Mamadou Konate & Zia Razzaq
Old Dominion University, United States

Abstract- This paper presents the outcome of a study of an I-section Glass Fiber Reinforced Polymer (GFRP) beam including retrofitting for damage effects. A total of three beam tests were conducted in the following sequence: GFRP beam with no retrofitting and a single mid-span web brace; the partially damaged (cracked) beam with GFRP plates used for retrofitting; and the retrofitted beam re-tested with the lateral brace at the top flange level. Both cracking and lateral-torsional buckling behavior is studied and experimental load-deflection relationships recorded. Using the mechanical properties of GFRP based on the experimental data, theoretical predictions are made for the buckling load values. The results show that retrofitted damaged beam provided about half of the original strength of the undamaged beam. The study also shows that the mid-span brace played a significant role in beam behavior and strength.

Keywords: I-section GFRP, retrofitting, lateral bracing.

GJRE-E Classification : FOR Code: 090599

BEHAVIOROFISECTIONGFRPBEAMINCLUDINGRETROFITTINGFORDAMAGEEFFECTS

Strictly as per the compliance and regulations of :

Behavior of I-Section GFRP Beam Including Retrofitting for Damage Effects

Mamadou Konate [α] & Zia Razzaq [σ]

Abstract- This paper presents the outcome of a study of an I-section Glass Fiber Reinforced Polymer (GFRP) beam including retrofitting for damage effects. A total of three beam tests were conducted in the following sequence: GFRP beam with no retrofitting and a single mid-span web brace; the partially damaged (cracked) beam with GFRP plates used for retrofitting; and the retrofitted beam re-tested with the lateral brace at the top flange level. Both cracking and lateral-torsional buckling behavior is studied and experimental load-deflection relationships recorded. Using the mechanical properties of GFRP based on the experimental data, theoretical predictions are made for the buckling load values. The results show that retrofitted damaged beam provided about half of the original strength of the undamaged beam. The study also shows that the mid-span brace played a significant role in beam behavior and strength.

Keywords: I-section GFRP, retrofitting, lateral bracing.

I. Introduction

Glass fiber reinforced polymer (GFRP) composites are increasingly been used for civil and mechanical structures. Under real-life use, situations can arise where a damaged GFRP structure needs to be retrofitted to restore all or a significant portion of its original strength. The damage could be a result of accidental overloading, misuse, or environmental conditions. A number of papers have previously been published about reinforced concrete structures retrofitted with GFRP composites [1, 4, 5, 11, 14]. This paper presents the outcome of a study of retrofitting a GFRP beam with GFRP plates.

a) Problem Statement

This investigation details an experimental and theoretical study of bending and lateral-torsional buckling of an I-section GFRP beam first loaded to its maximum load capacity, and then retrofitted with GFRP and re-tested. The beam has shear-type boundary conditions and mid-span lateral bracing. In each case, the beam is subjected to a gradually increasing mid-span load P until it reaches its maximum load-carrying capacity. The small moment resistance of the shear type steel end connections is considered to be negligible. The main objectives of this paper are to both experimentally and analytically investigate the cracking loads for a GFRP beam with and without GFRP retrofitting including lateral torsional buckling effects. Figure 1 shows the schematic of the GFRP beam of length L studied herein.

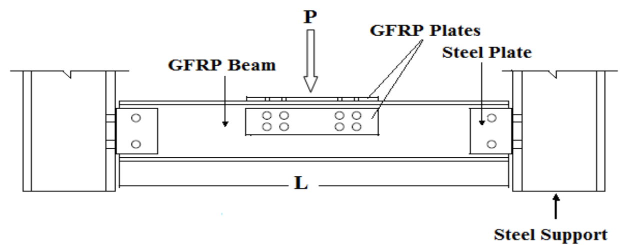

Fig. 1 : Schematic of GFRP beam

A three-fold problem has been studied in the present paper. First, the behavior of a GFRP beam with no retrofitting and a single mid-span web brace is studied. Next, the partially damaged beam with mid-span web brace is retrofitted with GFRP plates and its behavior observed. Lastly, the GFRP beam is re-tested, however with the mid-span brace provided at the top flange level. A comparison of the experimental peak loads is also made to those obtained with approximate analysis. Figure 2 shows the cross section with two alternative mid-span brace locations. Often one or more lateral braces are provided in order to increase the load-carrying capacity of a GFRP beam. The ultimate load is also influenced by whether a lateral brace is provided on the web or top flange. A comparison of the experimental peak loads is also made to those obtained with approximate analysis.

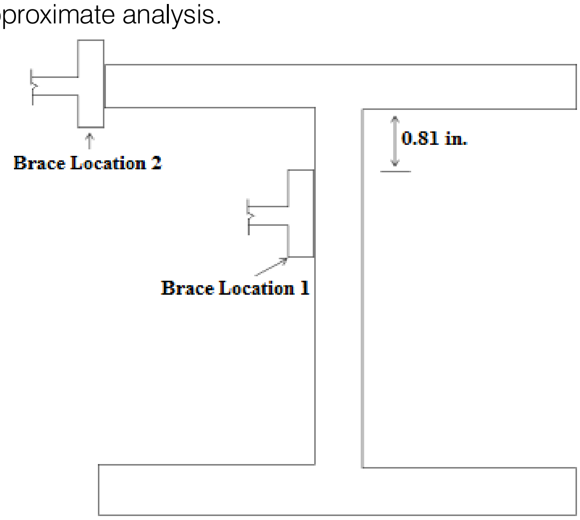

Fig. 2 : Cross section with alternative mid-span brace locations

Author α: Research Assistant, Department of Civil and Environmental Engineering, Old Dominion University, Virginia, USA.
e-mail: cvkonate@gmail.com
Author σ: University Professor, Department of Civil and Environmental Engineering, Old Dominion University, Virginia, USA.

II. Experimental Investigation

Three experiments are conducted using a GFRP beam with a clear length of 93 inches. The damaged GFRP is retrofitted with GFRP in the last two experiments. The load-deflection curves and the peak loads are recorded. Figure 3 shows the experimental test setup. In this figure, a dial gage (DG4) is also shown which is used to record the mid-span vertical deflection. A total of seven dial gages were mounted to record both vertical and lateral deflections. A hydraulic jack of 50-kip capacity with load cell and a loading device are also shown in Figure 3.

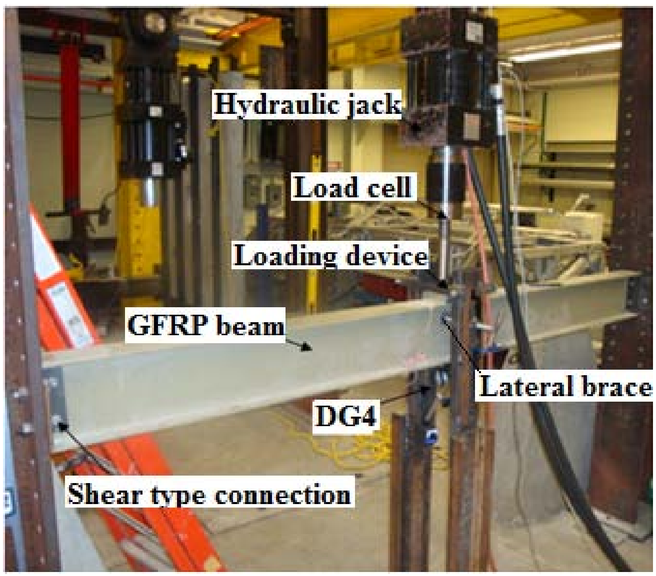

Fig. 3 : Experimental test setup

The hydraulic jack is controlled by the system console. This arrangement gradually transmits load from the hydraulic jack to the GFRP beam. The test procedure involved applying the load, P, in small increments and recording the resulting deflections. The loading process is continued until the member's load-carrying capacity is reached.

a) Beam with Mid-span Lateral Brace on Web

The mid-span web brace is provided on both sides of the web at 0.81 in below the bottom surface of the top flange. When approaching failure, the GFRP beam first buckled and then cracked. Figure 4 shows the view showing the top flange cracks and length of the GFRP beam. The buckling mode observed in the horizontal plane was S-shaped. The beam developed lateral-torsional buckling at a load of 8,426 lbs, and subsequently cracked at a load of 8,542 lbs. The beam exhibited elastic behavior up to the attainment of buckling load. Figure 5 shows the beam load-deflection curves of the GFRP beam for the lateral deflection (DG2) and the vertical deflection (DG3) both at the beam quarter length from the left support, and for the mid-span deflection (DG4).

Fig. 4 : Top flange GFRP beam cracking in Experiment 1

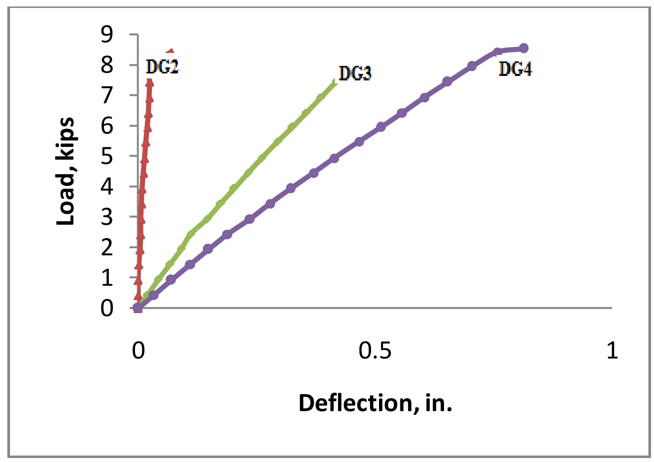

Fig. 5 : Load-deflection relations for Experiment 1

b) Damaged and Retrofitted GFRP Beam with Mid-span Brace on Web

The GFRP damaged beam from Experiment 1 is first retrofitted with CFRP plates on both sides of the web and top flange and then re-tested. Figure 6 shows the GFRP plates used to retrofit the mid-span top flange and two sides of the web, respectively. The plates were 0.5-inch thick and mounted to the beams using 0.875-inch diameter steel bolts.

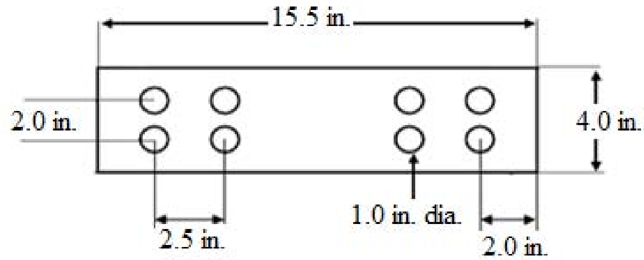

a) GFRP plate at mid-span top flange

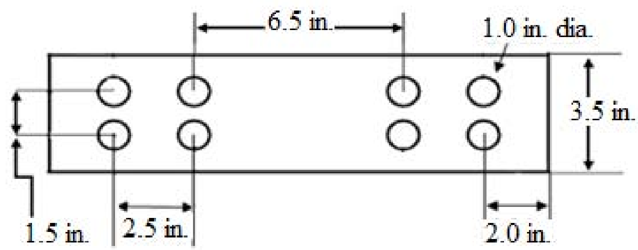

b) GFRP plate at both sides of mid-span web

Fig. 6 : GFRP retrofitting plates used at mid-span

Figure 7 shows a part of the retrofitted beam for Experiment 2. For Experiment 2, the arrangement for the dial gages, mid-span web brace Location 1 indicated in Figure 2, the applied load location, and the beam end connection remain the same as for Experiment 1. The resulting load-deflection curves for Experiment 2 are shown in Figure 8 showing a buckling load of 3,910 lbs.

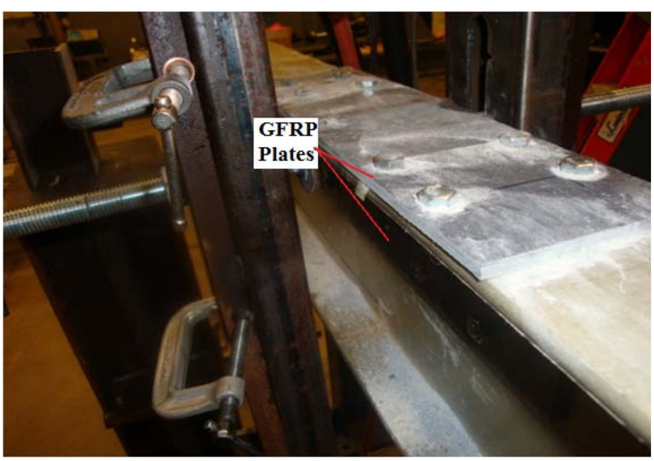

Fig. 7 : Retrofitted damaged beam

c) Residual Strength of Retrofitted Damaged Beam with Mid-span Brace on Top Flange

The damaged GFRP beam with GFRP retrofitting tested in Experiment 2 is tested again in Experiment 3 in which the mid-span braces are located at the top flange indicated as Location 2 in Figure 2. In this experiment, the beam buckled at a load of 4,372 lbs. The load in Experiment 3 is approximately 12 percent greater than that found in Experiment 2 indicating a greater effectiveness of the brace at the top flange as compared with the one on the web. Figure 9 shows the load-deflection relations obtained for Experiment 3.

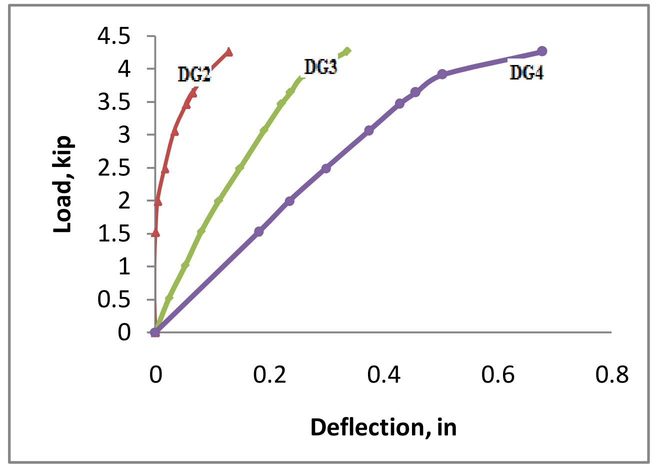

Fig. 8 : Load versus deflection relations for Experiment 2

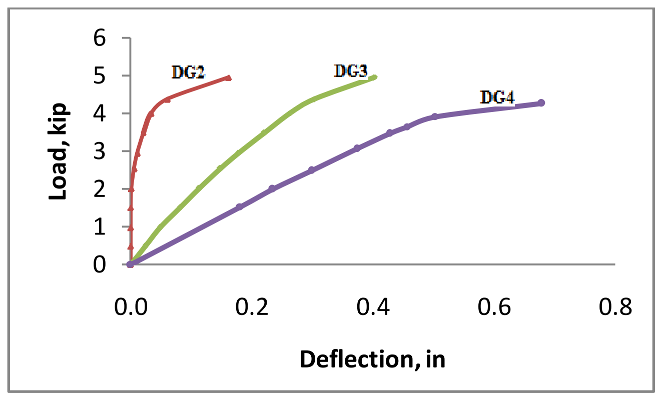

Fig. 9 : Load versus deflection relations for Experiment 3

III. Analysis and Comparison of Results

The following deflection equation from Reference 13 is used to calculate the longitudinal modulus of elasticity, E_{11}:

$$\Delta = \frac{PL^3}{48E_{11}I} \quad (1)$$

In this equation, P and Δ are obtained from the load-deflection curves for each experiment in the linear range. These values are also used to calculate the relative stiffness values, K. The value of the shear modulus is estimated using the following ratio [8]:

$$\frac{G_{12}}{E_{11}} = \frac{1}{8} \quad (2)$$

Table 1 presents the elastic limit load and deflection for each experiment, the relative stiffness values, the calculated modulus of elasticity, and the estimated shear modulus, respectively. The results shown in this table reveal that GFRP beam with mid-span lateral brace on web appeared to be much stiffer with K = 11,354 lbs/in. compared to both retrofitted damaged GFRP beam with mid-span web brace (K = 7,915 lbs/in.) and re-tested retrofitted damaged GFRP beam with flange brace (K = 8,922 lbs/in.). The K values also indicate that the retrofitted damaged GFRP beam with mid-span top web brace has a smaller stiffness than that of re-tested retrofitted damaged GFRP beam with mid-span flange brace.

Table 1 : Loads, Deflections, Stiffness, E11 and G_{12}

Experiment	P lbs	Δ in.	$K = \frac{P}{\Delta}$ lb/in	E_{11}x10^6 psi	G_{12}x10^6 psi
1	7948	0.7	11354	2.33	0.29
2	3641	0.46	7915	1.88	0.23
3	4372	0.49	8922	1.94	0.24

If $E_{11} = E_x$, the modified E_y can be calculated based on an averaged ratio $\lambda = \frac{E_y}{E_x}$ which is found to be 0.6 using the GFRP material properties given in Reference 8. The beam lateral-torsional buckling moment, M_{cr}, is calculated using the following equation [8]:

$$M_{cr} = C_b \frac{\pi}{kL_b} \sqrt{(\frac{\pi E_y}{kL_b})^2 C_w I_y + E_y I_y G_{12} J} \quad (3)$$

In this expression, C_w = warping constant (in^6); J = torsional constant (in^4); C_b = moment gradient multiplier; L_b = unbraced length (in); k = effective length coefficient; and I_y = moment of inertia about the minor axis. Table 2 presents the predicted lower, upper bound, and interpolated approximated buckling loads designated as P_L, P_U, P_{IB}, and P_{IU} respectively, for the three cases both with and without mid-span web brace. The lower bounds loads were found by neglecting the GFRP retrofitting plates in the cross-section properties calculations. The upper bound loads were calculated as if the retrofitting plates existed for the entire length of the beam. Also, for the theoretical buckling load calculations corresponding to Experiments 2 and 3, it was assumed that the beam is un-cracked. Presented in Table 2 are also the interpolated approximate theoretical buckling loads P_{IB} and P_{IU} calculated by using the upper and lower bound estimates for the buckling loads. The interpolation is done by using a weighted average involving the retrofitted and non-retrofitted portions of the beam length, namely, 15.5 in., and 77.5 in., respectively. For example, P_{IB} for the beam in Experiment 2 is calculated as follows:

Table 2 : Theoretical Lower and Upper Bound and Interpolated Buckling Loads

	Buckling Load (lbs) with brace			Buckling Load (lbs) without brace		
Exp	P_L lbs	P_U lbs	P_{IB} lbs	P_L lbs	P_U lbs	P_{IU} lbs
1	8148	12702	8907	1040	1545	1124
2	2670	4995	3058	409	608	442
3	3330	5191	3640	425	631	459

$$P_{IB} = [15.5(4995) + 77.5(2670)]/93.0 = 3058 \text{ lbs}$$

The beam in Experiment 1 was not retrofitted, however, the upper bound and interpolated buckling loads are still included in Table 2 to determine the theoretical effect of retrofitting. The results in Table 2 also clearly show that adding a brace at the beam mid-span results in a dramatic increase in the buckling load capacity.

Table 3 summarizes a comparison between theoretical estimates (P_t) for the buckling loads and those determined experimentally (P_e). Since no retrofitting was used for Experiment 1, the P_L value from Table 2 is taken as its P_t value in Table 3. The P_{IB} values corresponding to Experiments 2 and 3 from Table 2 are taken as their respective P_t values in Table 3. Both theoretical and experimental investigation revealed a reasonable agreement between the theoretically estimated and experimental buckling load values for Experiment 1. However, for Experiments 2 and 3, there was a difference of about 20 percent between the predicted loads and the experimental ones. This may be attributable to the complex nature of the retrofitted beam behavior with pre-existing cracking that Experiment 1 created. All of the predicted load values, however, are found to be on the conservative side.

Table 3 : Predicted and Experimental Loads

Experiment	P_t lbs	P_e lbs	P_t/P_e lbs
1	8148	8426	0.97
2	3058	3910	0.78
3	3640	4372	0.83

IV. Conclusions

A number of conclusions are drawn based on the results presented in this paper. The damaged or cracked GFRP beam retrofitted with GFRP plates carried nearly 46 percent of the load capacity of the originally undamaged GFRP beam without retrofitting but with the same mid-span web brace location. The re-tested and retrofitted GFRP beam with a mid-span brace at the top flange carried nearly 52 percent of the load carried by the originally undamaged GFRP beam. The mid-span lateral bracing played a significant role in the beam behavior and strength. Placing a lateral mid-span brace at the compression flange location results in a higher buckling capacity compared to that obtained using web bracing. Lastly, the results show that the use of lateral bracing dramatically increases the buckling capacity of the beam in comparison with that without the bracing.

References Références Referencias

1. Hamid, S., and Ehsani, M.R., "RC Beams Strengthened with GFRP Plates", *Journal of Structural Engineering*, Vol.117, No.11, November 1991, pp.3417-3433.
2. Meier, U., and Deuring, M., "Strengthening of Structures with CFRP Beams and Laminated", Research and Applications in Switzerland, 1st Intl. Conf. on Advanced Composite Materials in Bridges and Structures, 1992, p. 243, Sherbrooke, Canada.
3. Razzaq, Z, Prabhakaran, R., and Sirjani, M. B. "Load and Resistance Factor Design (LRFD) Approach for Reinforced-Plastic Channel Beam Buckling Composites" Engineering International Journal, Part B, 27 B, Great Britain, 1996, pp.361-369.
4. Phalguni, M., Narayan, S., and Cyril, L., "Optimizing Structural Response of Beams Strengthened with GFRP Plates", *Journal of Composites for Construction*, Vol.2, May 1998, pp.87-95.
5. Teng, J.G., Lam, L., Chan, W., and Wang, J., "Retrofitting of Deficient RC Cantilever Slabs Using GFRP Strips", *Journal of Composites for Construction*, Vol.4, No.2, May 2000, pp.75-84.
6. Loudon, N., "Strengthening Highway Structures with Fiber Reinforced Composites", Concrete, June 2001, pp.16.
7. Borri, A., Corradi, M., "New Materials for Strengthening and Seismic Upgrading Interventions", International Workshop Ariadne 10, Arcchip, Prague, Czech Republic, April 22-28 2002.
8. New and Improved Pultrex Pultrusion Desgn Manual of Standard and Custom Fiber Reinforced Polymer Structural Profiles, 2004 Edition, Volume 4-Revision 9.
9. Razzaq, Z, and Sirjani, M. B., "Stability of FRP Beams under Three-point Loading and LRFD Approach", Journal of Reinforced Plastics and Composites, Vol.24, No. 18, 2005.
10. Meier, U. and Stöcklin, I., "A Novel Carbon Fiber Reinforced Polymer (CFRP) System for Post-Strengthening", International Conference on Concrete Repair, Rehabilitation and Retrofitting (ICCRRR), November 2005, Cape Town, South Africa.
11. Raju, P.P., Tharun, D., and Bala, C.V.M., "Experimental Evaluation of Retrofitted Concrete Beams using CFRP and GFRP", *International Journal of Earth Sciences and Engineering*, Vol.04, No.06, October 2011, pp.812-818.
12. American Institute of Steel Constructon Inc., *Steel Construction Manual*, 14th Edition, 2011, Chicago.
13. Gene, J. and Goodno, B., "Mechanics of Materials", *8th Edition*, Thomson Books/Cole., United States, 2012.
14. Shinde, D.N., Pudale, Yojana. M., and Nair, Veena. V., "Flexural Behaviour of Reinforced Cement Concrete Beam Wrapped with GFRP Sheet", *International Journal of Research in Engineering and Technology*, Vol.03, No.03, May 2014, pp.760-763.

This page is intentionally left blank